

An overview of the impact of the January 10-11, 1997 magnetic cloud on the magnetosphere via global MHD simulation

C. C. Goodrich¹, J. G. Lyon², M. Wiltberger³, R. E. Lopez¹ and K. Papadopoulos³

Abstract. The results of a 3D MHD simulation of the January 10-11, 1997 geomagnetic storm are presented. The simulation results agree well with ground-based and geosynchronous observations. The 28 hours modeled by the simulation include the magnetic cloud responsible for the storm, the shock preceding the cloud, and the dense plasma filament following it. The simulation shows that during the period of southward IMF ionospheric activity was strongly correlated to the solar wind density. The arrival of the plasma filament during northward IMF pushed the dayside magnetopause well within geosynchronous orbit, but generated little ionospheric activity. It appears that n_{sw} as well as the orientation of B_{sw} plays a role in controlling the intensity of ionospheric and magnetospheric activity.

Introduction

On January 10, 1997, a magnetic cloud produced a major geomagnetic storm. This storm was the first solar terrestrial disturbance followed from its solar source through its consequences in the magnetosphere and ionosphere using the entire suite of resources of the International Solar Terrestrial Physics (ISTP) program. The SOHO LASCO experiment observed the CME expanding from the solar surface apparently toward the Earth on January 6. Early on January 10, WIND first observed the (CME associated) magnetic cloud, which produced a magnetic storm lasting 22 hours.

The WIND solar wind parameters are shown in Figure 1. A shock, observed at 0050 UT, preceded the magnetic cloud by about 4 hours. B_{sw} was generally northward following the shock passage, but turned southward twice for significant periods before the arrival of the magnetic cloud itself at about 0440 UT. During the 22 hour passage of the cloud, B_{sw} was strong (>15 nT) and smoothly rotated from due southward to northward. The cloud was followed by a dense plasma filament, in which n_{sw} increased to over 180 cm^{-3} by 0100 UT January 11.

We present here the results of a 3-D MHD magnetospheric simulation of the January 10-11 event, performed with the

¹Department of Astronomy, University of Maryland, College Park, MD.

²Department of Physics, Dartmouth College, Hanover, NH

³Department of Physics, University of Maryland, College Park, MD.

Lyon-Fedder-Mobarry code. The simulation, driven by WIND plasma and field data, models 28 hours of real time, from 0000 UT January 10 to 0400 UT January 11. While giving an overview of the full event, we will focus on the initial hours following the arrival of the magnetic cloud (0500-1200 UT), when B_{sw} was strongly southward, and the impact of the dense plasma filament following the cloud. We find the plasma density plays an important role in controlling magnetospheric and ionospheric activity during the period of southward B_{sw} .

Code Description

The Lyon-Fedder-Mobarry 3D MHD simulation code [e.g., Fedder and Lyon, 1995] models the solar wind and the magnetosphere beyond $2-3 R_E$ by numerically solving the ideal MHD equations. Similar approaches have been explored by other investigators [e.g., Walker et al., 1988]. The outer boundaries are at $x=30$ and $-300 R_E$ and $(y^2 + z^2)^{1/2} = 100 R_E$ and the inner boundary is at $r = 2R_E$. The simulation was performed in the Solar Magnetic (SM) coordinate system allowing the rotation of the earth's magnetic dipole to be included. Outflow conditions were applied on the rear (tailward) boundary where the plasma flow is supersonic. Elsewhere, external boundary conditions were specified using WIND solar wind data propagated appropriately to points on the front and cylindrical sides of the grid.

The application of the WIND data to the grid boundaries sets the registration of simulation time to actual (UT) time. We applied a constant propagation delay of 23 minutes to the WIND data, calculated using the average position of WIND (approximately $90 R_E$) upstream during the event and assuming an average solar wind speed of 410 km/s . This calculation neglects plasma and field evolution, propagation

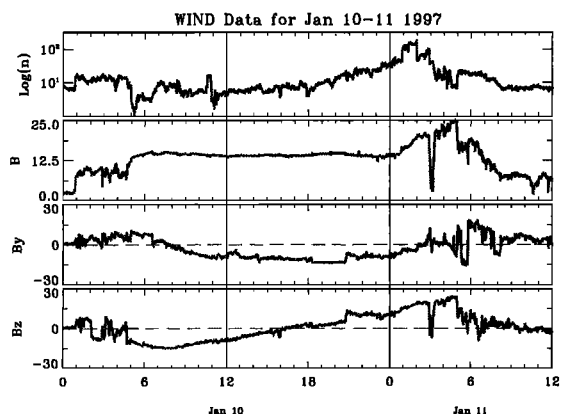


Figure 1- Solar wind magnetic field and plasma parameters from the WIND spacecraft

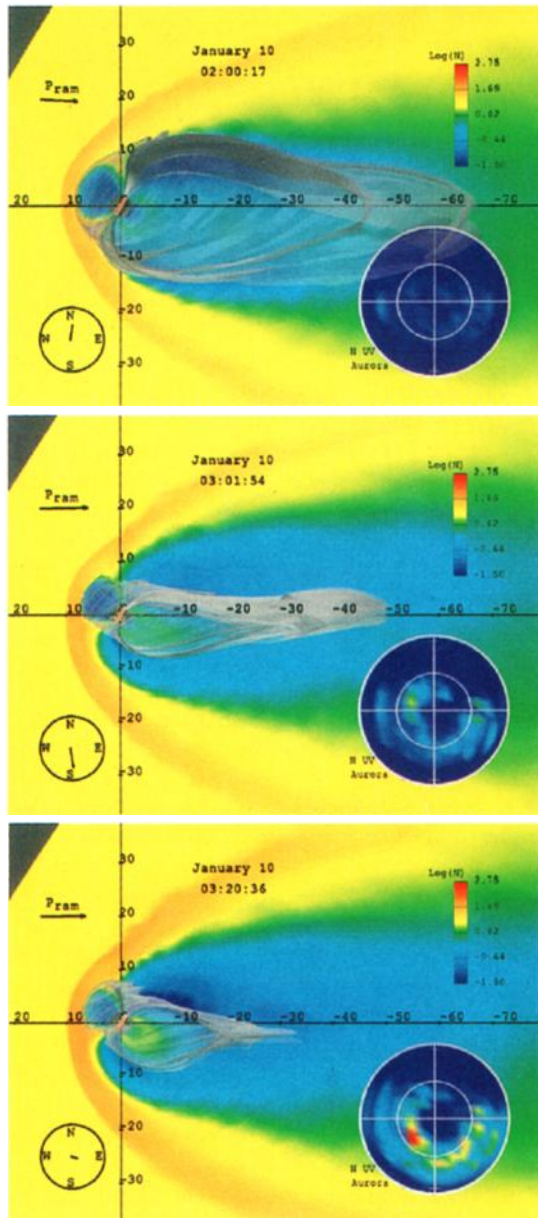


Figure 2 $-\text{Log}(n_{sw})$ in the noon-meridian plane, the open-closed field boundary (translucent 3D surface) are shown at (a) 0244, (b) 0300, and (c) 0315 UT. UV emission in the northern hemisphere ($>45^\circ$ Latitude), calculated from the simulation, is shown in MLT at lower left; noon is at the top of the insert. The upstream IMF direction and magnitude (compass arrow) and P_{ram} (vector) are also indicated.

of plasma structures as well as variations in V_{sw} , which can significantly affect the time registration over the 28 hours of the simulation. We estimate that the uncertainty in the time is between 10 to 15 minutes.

0100-0500 January 10

At the beginning of Jan 10, the simulation produced an essentially closed magnetosphere, with little open polar cap flux. It had an extended tadpole like shape, similar to that reported by Fedder and Lyon [1995]. Figure 2a shows the

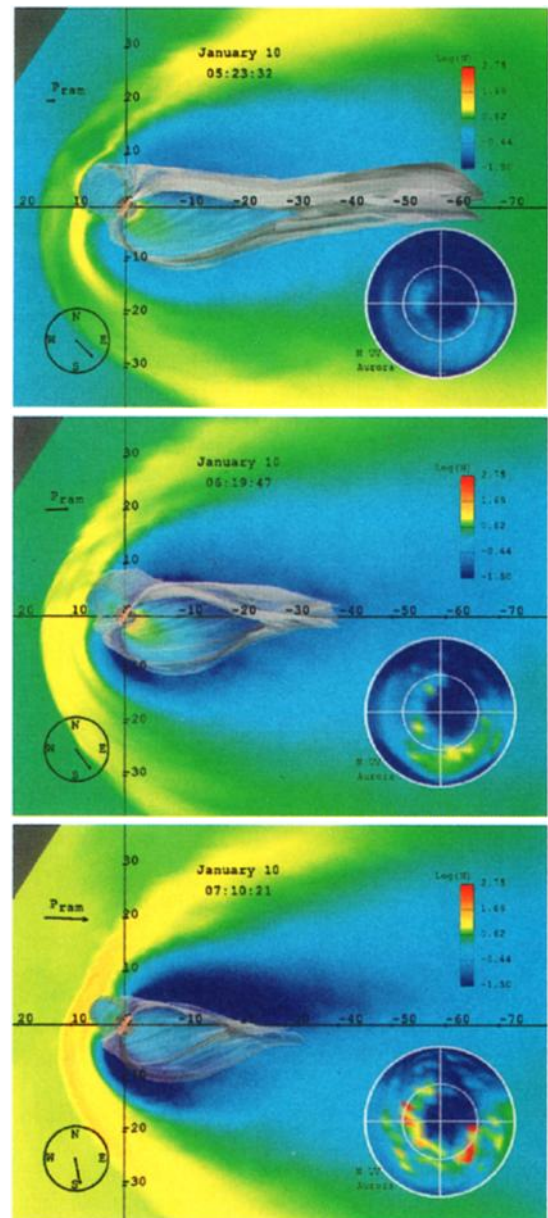


Figure 3 – Simulation results for (a) 0531, (b) 0618 and (c) 0710 UT on Jan 10 in the same format as Figure 2.

magnetospheric structure at 0200 UT, which is typical of 0100-0245 UT. The Figure shows the boundary of the closed field region as a 3D translucent surface, as well as the value of $\log(n)$ in the X-Z plane. There was essentially no ionospheric activity in the simulation at this time, as can be seen in the lower right corner of the Figure, where predicted UV emission [Fedder et al., 1995], proportional to the local field-aligned current density, is plotted.

The first significant activity followed the southward turning of B_{sw} (0250 UT) which led to a modest substorm with onset at about 0315 UT. Figure 2b shows the magnetosphere during the substorm growth phase at 0301 UT. Note the inward motion of the dayside bowshock and magnetopause, the increased flaring, and the thinning of the closed field region. The development of intense Region 1 currents can be seen in the ionospheric emission as well. After onset the simulation

developed vigorous reconnection of open flux at around $30 R_E$, resulting in an unloading of tail flux, a reduction in the polar cap size, and considerable auroral activity, as shown in Figure 2c. The ionospheric emission from the current wedge was just slightly before midnight at about 69° magnetic latitude. The magnetosphere subsequently expanded to a more relaxed state similar to that in Figure 2a between 0340 and 0410 UT. There was a weaker substorm with onset about 0440 UT that follows qualitatively the same pattern.

These results agree generally with the UV imager data available from POLAR [G. Parks, personal communication, 1998]. The UV images show the first onset occurred at about the same place in the ionosphere as predicted by the simulation, but about 20 minutes later (0336 UT) than in the simulation. The POLAR data, however, show continued activity for the following hour, in contrast to the two separate activations seen in the simulation.

0500-1500 UT January 10

The arrival of the magnetic cloud was marked by an abrupt southward turning and an increase in B_{sw} . The cloud's arrival was also marked by a large reduction of n_{sw} and T_{sw} at about 0510 UT. The large decrease in ram pressure caused the magnetopause and bow shock to move outward. Figure 3a, in the same format as Figure 2, shows the magnetosphere and ionospheric UV emission during the growth phase (0523 UT). At onset (0613 UT), a modest current wedge developed between midnight and 0100 MLT at about 62° magnetic latitude. Figure 3b (0618 UT) is shortly after the onset, as determined by a reduction of the amount of open polar cap flux.

The similarity of Figures 2(b-c) and 3(a-b) show that the arrival of the cloud initiated a substorm sequence much like the two preceding ones. The late growth phase configuration at 0523 UT in Figure 3a is similar to that in Figure 2b, but significantly less compressed due to the reduced ram pressure. The onset at about 0613 was considerably weaker, despite the strong southward field, as seen in the UV emissions in Figures 3b and 2c.

The sustained driving caused by the strongly southward B_{sw} did not allow a subsequent relaxation of the magnetosphere following the onset at 0613 UT. The magnetospheric structure and modest level of ionospheric emission (Figure 3b) is typical of the simulation produced until just before 0700 UT. The simulated magnetosphere appeared to reach a rough equilibrium state in which the rate of (strong) dayside merging was balanced by the rate of reconnection of lobe field in the tail.

Just before 0700 UT the solar wind density abruptly doubled, increasing the ram pressure and compressing the magnetosphere as seen in Figure 3c. The increased emission caused by the compression, shown in Figure 3c, occurred in a broad arc across the nighttime ionosphere, though greater in general in the post midnight sector. After 0710 UT the magnetosphere appeared generally to reach another, though more highly stressed, equilibrium in which the energy throughput was greater than before the density increased. The magnetospheric structure and ionospheric activity seen in Figure 3c are representative of the simulation while B_{sw} remained strongly southward. On a finer time scale, however, the equilibrium was only roughly in balance. In response to large density variations between 0700 and 1200 UT, the tail reconnection region moved abruptly and continually within –

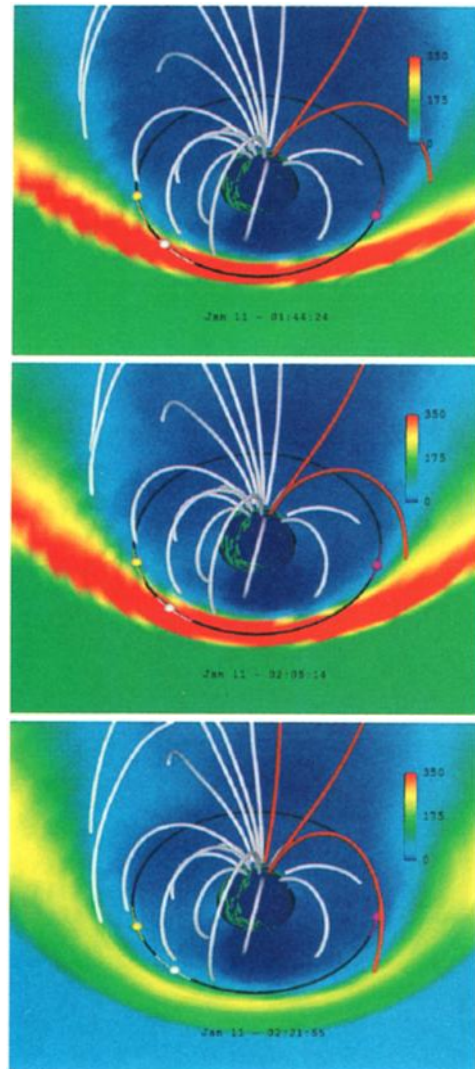


Figure 4 – Views of the plasma density in the equatorial plane at (a) 0144 UT and (b) 0205, and (c) 0245 UT on January 11 with closed (white) and open (orange) field lines. The black circle depicts geosynchronous orbit. The Earth is magnified by factor of 2, while preserving the geographic location of the magnetic field foot points, for clarity.

20 and $-30 R_E$, and the rate of reconnection varied. The ionospheric activity, which was primarily in the post-midnight sector, was modulated by the density variations as well, with significant intensifications correlated with the density pulses at 0730, 0840, and 1100 UT. This corresponds to the fact that the large perturbations recorded by the CANOPUS magnetometers (not shown) began around 0700 UT [G. Rostoker, personal communication, 1998], and that intensifications of activity occurred at roughly the times mentioned above.

1500 January 10 – 0300 January 11

From 1500 UT through the early hours of January 11, B_{sw} became steadily more northward. In response the driven magnetotail and ionospheric activity gradually subsided. However, beginning about 2200 UT, n_{sw} started to increase

first slowly, then abruptly at 0100 UT the next day to over 100 cm^{-3} , and 20 min later to 180 cm^{-3} . The enormous increase in P_{ram} compressed the entire magnetosphere, and moved the dayside magnetopause well within geosynchronous orbit by 0144 UT. Unlike the density impulse described above, this more massive density impulse during northward \mathbf{B}_{sw} produced minimal ionospheric activity in the simulation.

In Figure 4 we have indicated the positions of the LANL 1994-084 (white), 1991-080 (yellow), and the GOES 9 (orange) satellites. At 0144 UT the magnetopause in the simulation had been pushed inward of LANL 1994-084, which stayed in the magnetosheath until 0221 UT. LANL 1991-080 and GEOS 9 remained within the magnetosphere. Reeves *et al.* (1998) have reported that LANL 1994-080 actually entered the magnetosheath 10 minutes later at 0154 UT and remained there until 0217 UT. Furthermore GOES 9 and LANL 1991-080 remained in the magnetosphere, though the latter approached, but did not cross the magnetopause, at 0212 UT. The agreement with the simulation results is excellent, given the time registration uncertainty and finite spatial resolution of the code.

Summary

The simulation results show the importance of both the solar wind magnetic field and density in determining the structure of the magnetosphere and the activity in the ionosphere during the January 10-11, 1997 magnetic storm. The compression of the magnetosphere early on January 11 is not surprising. Simple pressure balance considerations explain the motion of the dayside magnetopause to well within geosynchronous orbit for more than 30 minutes. The simulation agrees quite well with the observations at geosynchronous orbit for this period.

The strong correlation we find between n_{sw} and ionospheric activity during the initial portion of the storm (0500-1500 UT) is of considerable interest. Statistical studies of substorm triggering have focused on the role of northward turnings of the IMF, but have not demonstrated significant correlations with solar wind density enhancements [Lyons, 1996, and references therein]. In the simulation, the lack of intense ionospheric activity for almost 2 hours after the southward turning at 0510 UT is clearly due to the unusually low density in this period. The beginning of intense activity at 0655 UT and the later intensifications at 0730, 0840, and 1100 UT are all due to significant density increases. This indicates the magnetosphere was strongly stressed and directly driven from 0500-1500 UT, and that the kinetic energy of the solar wind (not just the dayside merging rate) was a critical factor in determining the energy transfer from the solar wind to the magnetosphere.

This result is supported by the ground observations. The CANOPUS data [G. Rostoker, personal communication, 1998]

and the magnetometer data assembled by J-H. Shue and Y. Kamide [*Proceedings of the Fourth International Conference on Substorms, in press, 1998*] show the onset of intense ionospheric activity just before 0700 UT, as seen in the simulation. Sanchez *et al.* [1998] report increases in Pedersen conductivity and ion flows at this time in the Sonderstrom radar data. They find the activity to be relatively concentrated in the postmidnight sector, as it is in the simulation.

It is most likely that the correlation between n_{sw} and magnetospheric and ionospheric activity is due to a condition that characterized 0500-1500 UT on January 10 - unusually strong southward \mathbf{B}_{sw} . Previous studies may not have considered these extreme conditions. In fact, Shue and Kamide [1998] have calculated the correlation between n_{sw} and ionospheric activity in their collection of magnetometer data for January 10. They find little correlation before 0530 UT but a strong correlation thereafter. We suspect that the large amount of coupling between the solar wind and the magnetosphere during the southward phase of the cloud allowed a significant fraction of the incident solar wind kinetic energy to enter the magnetosphere. We intend to pursue this line of investigation through a more detailed examination of this and other events by means of simulation and comparison to observations.

Acknowledgements. We have benefited greatly in writing this paper from discussions with G. Rostoker, J-H. Shue, B. Tsutsumi, and A. Weatherwax. We also thank the Canadian Space Agency for the CANOPUS data and the Pittsburgh Supercomputer Center for computational resources. This work was supported in part by NASA grants NAG5-101, NAG5-4662, NAG5-6256, NAGW-3222, NAG5-2252, and NSF grant ATM-9527055.

References

- Coroniti, F. V., and C. F. Kennel, Can the ionosphere regulate magnetospheric convection?, *J. Geophys. Res.*, **78**, 2837, 1973.
- Fedder, J. A. and J. G. Lyon, The earth's magnetosphere is 165 RE long, *J. Geophys. Res.*, **100**, 3623, 1995.
- Fedder, J. A., S. P. Slinker, J. G. Lyon and R. D. Elphinstone, Global numerical simulation of the growth phase and expansion onset for a substorm observed by Viking, *J. Geophys. Res.*, **100**, 19083, 1995.
- Lyons, L. R., Substorms: Fundamental features, distinction from other disturbances, and external triggering, *J. Geophys. Res.*, **101**, 13011, 1996.
- Reeves, G. D., and R. H. W. Friedel, and R. D. Belian and M. M. Meier and M. G. Henderson and T. Onsager and H. J. Singer and D. N. Baker and Xi Li and J. B. Blake, The relativistic electron response at geosynchronous during the January 1997 magnetic storm, *Geophys. Res. Lett.*, (*this issue*), 1998.
- Sanchez, E. R. and J. P. Thayer and J. D. Kelly and R. A. Doe, Energy transfer between the ionosphere and the magnetosphere during the January 1997 CME event, *Geophys. Res. Lett.*, (*this issue*), 1998.
- Walker, R. J., T. Ogino and M. Ashour-Abdalla, A global magnetohydrodynamic model of magnetospheric substorms, in *Physics of Space Plasmas*, edited by T. Chang, G. B. Crew, and J. R. Jasperse, SPI CONF. Proc. Reprint Ser., **7**, 235, 1988.

(Received: November 6, 1997; Revised: March 19, 1998; Accepted: March 25, 1998.)